Molecular Crystals and Liquid Crystals Incorporating Nonlinear Optics
Publication details, including instructions for authors and subscription information:
http://www.tandfonline.com/loi/gmcl17

Quantitative SEM Characterization of Polymer-Dispersed-Liquid-Crystal Films

J. R. Havens [a], D. B. Leong [a] & K. B. Reimer [a]
[a] Raychem Corporation, Menlo Park, CA, 94025
Version of record first published: 04 Oct 2006.

To cite this article: J. R. Havens , D. B. Leong & K. B. Reimer (1990): Quantitative SEM Characterization of Polymer-Dispersed-Liquid-Crystal Films, Molecular Crystals and Liquid Crystals Incorporating Nonlinear Optics, 178:1, 89-101

To link to this article: http://dx.doi.org/10.1080/00268949008042711

Mol. Cryst. Liq. Cryst., 1990, Vol. 178, pp. 89–101
Reprints available directly from the publisher
Photocopying permitted by license only

Printed in the United States of America

Quantitative SEM Characterization of Polymer-Dispersed-Liquid-Crystal Films

J. R. HAVENS, D. B. LEONG, and K. B. REIMER
Raychem Corporation, Menlo Park, CA 94025

(*June 23, 1989*)

Large-area displays and light valves can be made by dispersing nematic liquid-crystal droplets in a polymer matrix. To switch between scattering and transparent states of the polymer film, an electric field is used to alter the refractive index of the droplets by changing the orientation of their liquid-crystal directors. The film morphology—by which we mean the size, shape, and spatial distribution of droplets in the polymer matrix—is thought to have an important influence on its electro-optical properties, but definitive relationships have proved difficult to establish. This paper discusses the application of scanning electron microscopy (SEM) to characterize the film morphology. We have developed a means of sample preparation which allows us to obtain representative cross sections of the liquid-crystal droplets dispersed in the matrix. We then transform the statistical information obtained through digitization of the images, so that droplets are counted on a volume, rather than an area, basis. While a quantitative theory has not yet been developed, the histogram of droplet sizes should correlate with the scattering cross section of the film per unit volume, an important electro-optical parameter for many applications.

INTRODUCTION

NCAP (Nematic Curvilinear Aligned Phase) films are comprised of nematic liquid-crystal (LC) droplets dispersed in a polymer matrix.[1] When placed between two transparent, conductive electrodes, such films can be made to undergo a transition between scattering and transparent states, by application of a suitable voltage. The electro-optical characteristics of NCAP films (contrast ratio, switching voltage, switching speed, etc.) make them attractive for use in large-area displays and light valves.[2] To optimize the performance of the films, we are studying the relationship between the electro-optical parameters and the construction details of the NCAP cells. In addition to material parameters such as the refractive indices of the constituents and the mechanical elasticity of the polymeric binder, the film morphology is thought to be an important determinant of the electro-optical performance. In this paper we focus on scanning electron microscopy (SEM) as a means to quantitatively characterize NCAP film morphology.

A representative cross section of an NCAP film is shown in Figure 1(a). Qual-

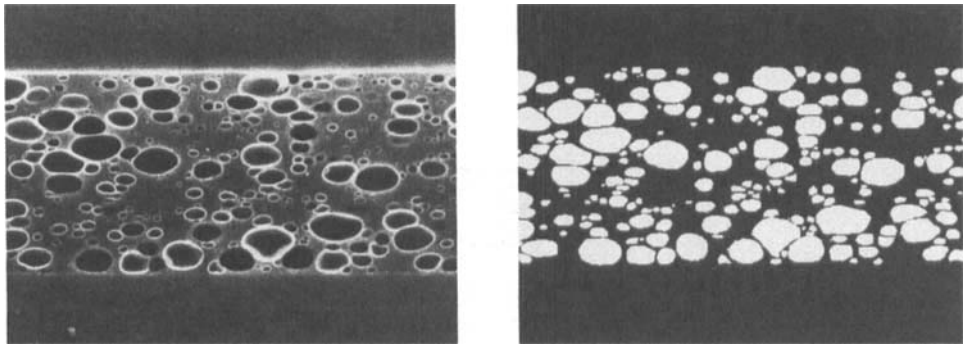

(a) (b)

FIGURE 1: *(a)* Representative cross section of an NCAP film. *(b)* Binary image of the micrograph in *(a)*, demonstrating how the LC droplets are counted.

itative differences among films can be discerned visually, if the differences are sufficiently striking; but for quantitative characterization of the film morphology, something else is needed. Our approach has been to generate a binary image of the SEM micrograph (*e.g.*, Figure 1(b)), in which pixels are turned either on or off depending on whether they are located within a liquid-crystal droplet. Image-processing programs can then be used to count droplets in the binary image. In this fashion we can obtain both the size distribution and shape of the droplet cross sections. It then becomes necessary to convert the information from size and shape per unit area to size and shape per unit volume. This accounts for the possibility that a large droplet in the film may be sectioned close to its surface and therefore appear to be small in the cross-section micrograph. It also accounts for the fact that small droplets in the volume are more likely to be missed entirely by the sectioning plane than are large droplets. Once the number of droplets per unit volume is known for all droplet sizes, then different histograms can be constructed—number percent, surface-area percent, and volume percent, for instance. Furthermore, moments of these distributions can be calculated, as a means of quantitatively characterizing the film morphology.

Through the availability of dedicated minicomputers and software, quantitative microstructural analysis of electron micrographs has recently grown in popularity. In the broad range of applications of quantitative microscopy,[3–6] we are interested in characterizing three-dimensional structures based on information from two-dimensional sections.[7–12] In particular, we require the size distribution of oblate ellipsoids from measurements made on planes parallel to the axes of revolution. To accomplish this, we have modified DeHoff's analysis of the size distribution of ellipsoidal particles from random plane sections[13,14] to obtain equations appropriate for the NCAP films. Our primary motivation is that the number of droplets of a given size per unit volume should relate well to the electro-optical properties of the films.

EXPERIMENTAL SECTION

NCAP Film Preparation

Polymer-dispersed-liquid-crystal films can be prepared in a variety of methods.[2,18–20] The NCAP films analyzed in this paper were generated by emulsifying a nematic liquid crystal in an aqueous solution of poly(vinyl alcohol) (PVA). The emulsions were then coated onto a conductive, transparent electrode (indium-tin-oxide-coated polyester) by drawing a knife edge just above the electrode surface. The films were then dried under ambient conditions, prior to lamination with another sheet of conductive substrate. This construction results in a finished NCAP cell.

Microtoming of NCAP Films

Creating undistorted cross sections of NCAP films is essential if accurate, quantitative characterization of the LC-droplet sizes is desired. After considerable experimentation with fracturing and cutting methods, we settled on the following procedure. The NCAP laminations are cut with a diamond knife at -196 C in a Reichert Ultracut E microtome, with an FC4D cryogenic attachment. While immersed in liquid nitrogen, the sectioned film is transferred to a vacuum evaporator, where the nitrogen is sublimed at pressures of 10^{-5} torr. The films are typically left under vacuum for a period of 16 hours, during which time they warm to room temperature in the absence of moisture. The samples are then sputter-coated with a thin layer of gold and examined in a JEOL Model 2000FX STEM, operated in the SEM mode.

Image Digitization and Analysis

The next step in the quantitative characterization is to generate a binary image from the video display of the SEM. The binary image is one in which pixels are either on or off, depending on whether they lie in a LC droplet or in the surrounding polymer matrix. It is most conveniently created through the use of a gray-scale-segmentation process, followed by careful editing to verify that each of the droplets in the video image is correctly treated. Human judgment is definitely required to generate accurate binary images for these films, since droplet boundaries may be incomplete or may display poor contrast. We exercised considerable care in generating the binary images, by comparing results frequently during editing with both video and photographic images of the films. Figure 1 shows representative images, before and after processing. A Tracor-Northern Model 5500 X-ray analyzer was used in the generation and analysis of the binary images of the NCAP films.

EQUATIONS FOR DROPLET-SIZE DISTRIBUTION

The electro-optical properties of NCAP films are known to be influenced by the size distribution of LC droplets. We would like to quantify such relationships, but

first must determine the number of LC droplets per unit volume as a function of the droplet size. The goal of the following analysis is to obtain this information from the SEM cross sections of a film. The major problems are immediately apparent: (1) a droplet may be sectioned anywhere; even a large droplet may give a small section, if it is cut far from its center; and (2) smaller droplets are more likely to be missed entirely by the sectioning plane. The gist of what follows is then the correction for the sectioning statistics.

Previous Work on Random Sections

Scheil[15] and Saltykov[16] pioneered work in this area by considering distributions formed by random plane sections through groups of spherical particles. DeHoff has expanded the calculations by dealing with random plane sections through ellipsoids of revolution.[13,14] By assuming that all ellipsoids in the sample have the same shape (*viz.*, the same ratio of minor- to major-axis length) and that the area examined is large enough to accurately represent the average of all possible random sections, DeHoff derives the following equation[13]:

$$n_i = k(q)\Delta \sum_{j=i}^{k} N_j \alpha_{i,j}. \tag{1}$$

To define the quantities in this expression, we must first recognize that both ellipsoids in the film and ellipses in the cross section are classified according to the lengths of their major axes. (This is appropriate for the case of oblate ellipsoids of revolution—the relevant case for NCAP films, as we will show shortly.) A histogram of LC-droplet sizes can then be divided into k bins, with the increment in size from bin to bin being defined by Δ. The maximum major-axis length for both ellipsoids and ellipses is therefore $k\Delta$. In Equation (1), n_i defines the number of ellipses per unit area in the cross section whose major-axis length lies between $(i-1)\Delta$ and $i\Delta$. Similarly, N_j specifies the number of droplets per unit volume in the film whose major axis length lies between $(j-1)\Delta$ and $j\Delta$. The quantity $k(q)$ represents a shape factor for random sectioning and is a function of q, the ratio of the minor- to major-axis of the ellipsoids (assumed to be independent of size). Whether the ellipsoids are prolate or oblate has a considerable effect on $k(q)$. Finally, $\alpha_{i,j}$ is given by an algebraic expression of the integral indices:

$$\alpha_{i,j} = \sqrt{j^2 - (i-1)^2} - \sqrt{j^2 - i^2}. \tag{2}$$

Equation (1) can then be inverted to yield

$$N_j = \frac{1}{k(q)\Delta} \sum_{i=j}^{k} n_i \beta_{j,i}, \tag{3}$$

where the $\beta_{j,i}$ form a matrix of coefficients.[13] Equation (3) is the desired form of the expression for droplet-size distribution, since the left-hand side is the number

of droplets of a given size per unit volume and the right-hand side can be determined from experimental data for the cross section.

NCAP Films

The situation with NCAP films is clearly different from that dealt with by DeHoff. Figures 1 and 2 demonstrate that the LC droplets are not randomly oriented with respect to the surface of the cut, and therefore DeHoff's assumption of random plane sections is not appropriate for this case. In what follows, we develop the relevant equations for obtaining the three-dimensional droplet-size distribution for NCAP films from two-dimensional cross-section data.

Assumptions

(1) The shapes of the LC droplets are well approximated by oblate ellipsoids of revolution.

(2) All droplets have the same orientation with respect to the NCAP-film surface. The minor axes of the ellipsoids are perpendicular to the electrode surface and are parallel to the cutting plane used to generate the cross section.

(3) Ellipsoids in a given size class are well approximated by the largest ellipsoid in that class.

Justification

Figure 2 shows an NCAP-film section prepared by microtoming parallel to the electrode surface and perpendicular to the direction used in Figure 1. The droplet cross sections are quite circular in Figure 2, which suggests that the liquid-crystal spheres present in the emulsion are flattened to oblate ellipsoids during the drying process. The figures also support *Assumption (2)*, in that almost all droplets have parallel minor axes. *Assumption (3)* allows us to deal with summations over a

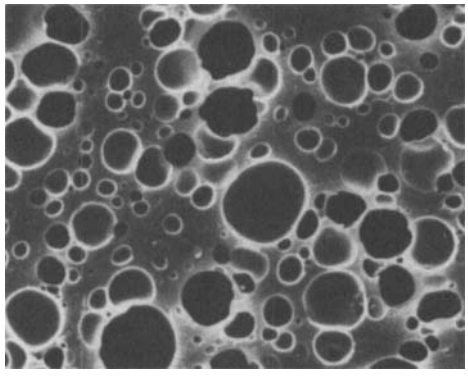

FIGURE 2: SEM micrograph of an NCAP film sectioned parallel to the electrode surface. When considered in conjunction with the ellipses shown in Figure 1(a), the circular cross sections seen here indicate that the LC droplets form oblate ellipsoids in the film.

manageable number of indices and is reasonable as long as $k \geq 10$ and $\Delta \leq 1$ micron. It permits presentation of the results in an easily interpretable histogram format.

One advantage of the NCAP geometry, relative to the random plane sections treated by DeHoff,[13,14] is that it is not necessary when calculating the number distributions to assume that ellipsoids of all sizes have the same shape, as characterized by the ratio of the minor to major axis, q. Such an assumption is more problematic than those listed above, since cross sections for the small droplets frequently appear to be somewhat more spherical than for the large ones. (We note that for the sectioning geometry specified by *Assumptions (1)* and *(2)*, q for the cross sections is identical to q for the three dimensional ellipsoids.) While having no effect on the number distribution, this variation introduces additional error into the surface-area and volume distributions, for which we do assume constant particle shape to simplify the summations.

Derivation

Consider a unit volume of NCAP film which contains N_j droplets characterized by major-axis length B_j. This volume is represented in cross section by a unit area which contains n_i ellipses with major-axis length b_i. Of these n_i ellipses, $n_{i,j}$ arise from the N_j droplets; the rest come from either larger or smaller droplet classes. Invoking *Assumption (2)*, we define ρ to be the distance between the center of an ellipsoid and the cutting plane which forms the cross section. More specifically, $\rho_{i,j}$ is the distance between one of the ellipses contributing to n_i and the center of its generating ellipsoid from the B_j class. All intersections which contribute to $n_{i,j}$ arise from ellipsoids whose centers lie between $\rho_{i-1,j}$ and $\rho_{i,j}$ either in front of or in back of the cutting plane. We define the total thickness of the slices in which these ellipsoid centers lie as follows:

$$T_{i,j} = 2(\rho_{i-1,j} - \rho_{i,j}). \tag{4}$$

We can now generate an expression for $n_{i,j}$:

$$n_{i,j} = T_{i,j}N_j = 2(\rho_{i-1,j} - \rho_{i,j})N_j. \tag{5}$$

At this point we need an equation for $\rho_{i,j}$ for oblate ellipsoids in the NCAP orientation. Consider an oblate ellipsoid of revolution centered at the origin and defined by the equation

$$\frac{x^2 + y^2}{\left(\frac{B_j}{2}\right)^2} + \frac{z^2}{\left(\frac{qB_j}{2}\right)^2} = 1, \tag{6}$$

in which B_j is the major-axis length and qB_j is the minor-axis length. The ellipse defined by the intersection of this ellipsoid with the cutting plane $x = \rho_{i,j}$ is given by

$$\frac{y^2}{\left(\frac{B_j}{2}\right)^2 - \rho_{i,j}^2} + \frac{z^2}{q^2\left(\left(\frac{B_j}{2}\right)^2 - \rho_{i,j}^2\right)} = 1. \tag{7}$$

This ellipse has a major-axis length b_i given by

$$\left(\frac{b_i}{2}\right)^2 = \left(\frac{B_j}{2}\right)^2 - \rho_{i,j}^2 \Rightarrow \rho_{i,j} = \frac{1}{2}\sqrt{B_j^2 - b_i^2}. \tag{8}$$

Substituting this expression for $\rho_{i,j}$ into Equation (5), we find

$$n_{i,j} = \left(\sqrt{B_j^2 - b_{i-1}^2} - \sqrt{B_j^2 - b_i^2}\right)N_j \tag{9}$$

$$n_{i,j} = \Delta N_j \alpha_{i,j}. \tag{10}$$

Summing over appropriate values of j, we have

$$n_i = \Delta \sum_{j=i}^{k} N_j \alpha_{i,j}, \tag{11}$$

which is the same as Equation (1), if the shape factor $k(q)$ is taken as unity. Therefore, the geometry of NCAP sectioning yields a result similar to that given by DeHoff for random sections on ellipsoids of constant shape[13] (*cf.*, Equation (3)):

$$N_j = \frac{1}{\Delta} \sum_{i=j}^{k} n_i \beta_{j,i}. \tag{12}$$

This is also the same equation proposed by Saltykov for random plane sections through spherical particles of different diameters.[16] The matrix of coefficients $\beta_{j,i}$ is identical as well. Since this matrix is known and since n_i and Δ are experimentally measured, N_j can be determined in a straightforward fashion. This accomplishes our goal of obtaining the droplet-size distribution per unit volume from micrographs of film cross sections.

RESULTS AND DISCUSSION

The number distribution of LC-droplet sizes in an NCAP film is shown in Figure 3, before and after treatment with the equations developed in the previous section.

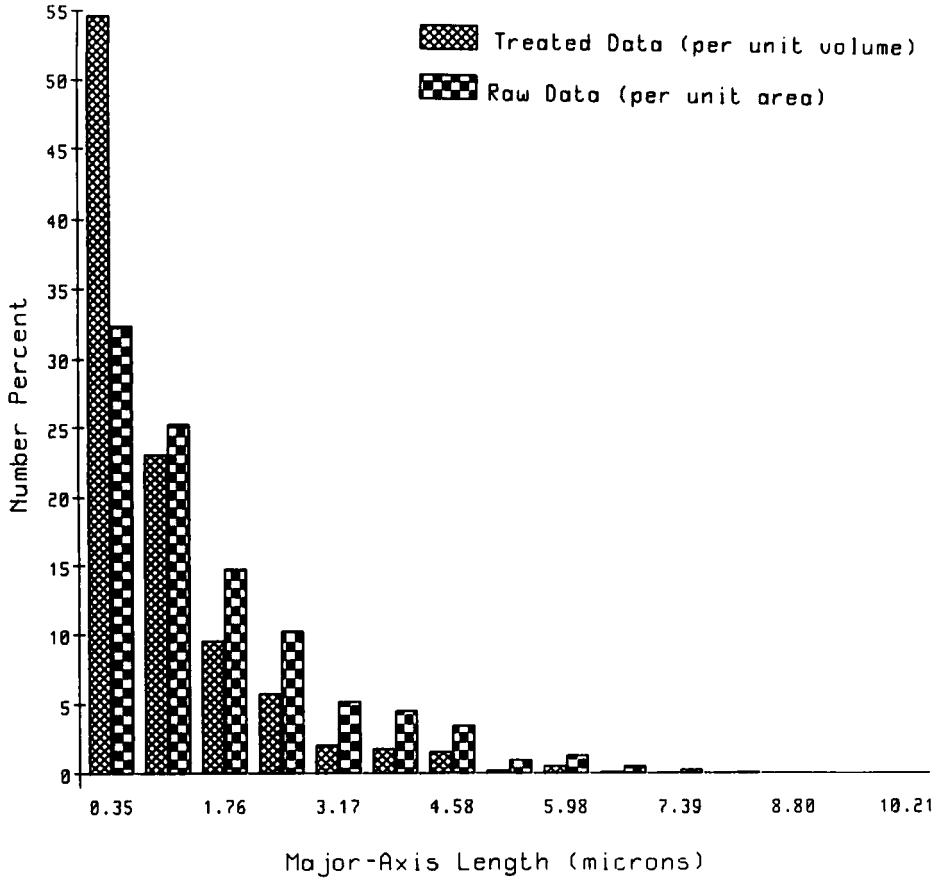

FIGURE 3: Histogram showing the conversion of SEM-cross-sectional data recorded in two dimensions to the number distribution of LC droplets per unit volume. This conversion relies on assumptions and matrix manipulations discussed in the text. The bin size for the abscissa is fixed by the major axis of the largest droplet measured; the numbers along the abscissa refer to the centers of the bins.

The raw data represent the distribution of ellipse major-axis lengths taken from SEM cross sections such as that shown in Figure 1. A total of 1322 droplets (with an average q of 0.69) was counted in the binary images, encompassing an area of approximately 12,000 square microns. The treated data represent the results from application of Equation (12) and give the size distribution of LC droplets per unit volume. (Numbers along the abscissa represent the center of each bin.) Both distributions show an essentially monotonic decrease in the number of droplets as the major-axis length increases from 0 to 10.57 μm, the size of the largest droplet present. In the treated data, however, there is a substantial increase in the number of droplets contributing to the smallest bin, between 0 and 0.70 μm. Two opposing effects contribute to the translation of the treated data relative to the untreated. First is the observation that large droplets sectioned close to their surfaces result

in relatively small ellipses. This effect causes a shift in the histogram to larger major-axis lengths upon conversion of the size distribution to a volume basis. On the other hand, small droplets which reside in a given unit volume have a greater chance of being missed entirely by the sectioning plane than do large droplets. This effect causes a shift to smaller major-axis lengths upon conversion to a volume basis. Apparently, this second effect dominates in the NCAP film studied here, as the number percent of droplets in the smallest bin (≤ 0.70 μm) rises from 33% per unit area to 55% per unit volume.

Figures 4 and 5 show the surface-area and volume distributions, respectively, both calculated on a volume basis. We feel it likely that these distributions will correlate better with macroscopic electro-optical properties of NCAP films than do either of the number distributions shown in Figure 3, but experimental data are incomplete at this point. (Since the refractive-index difference across the surface

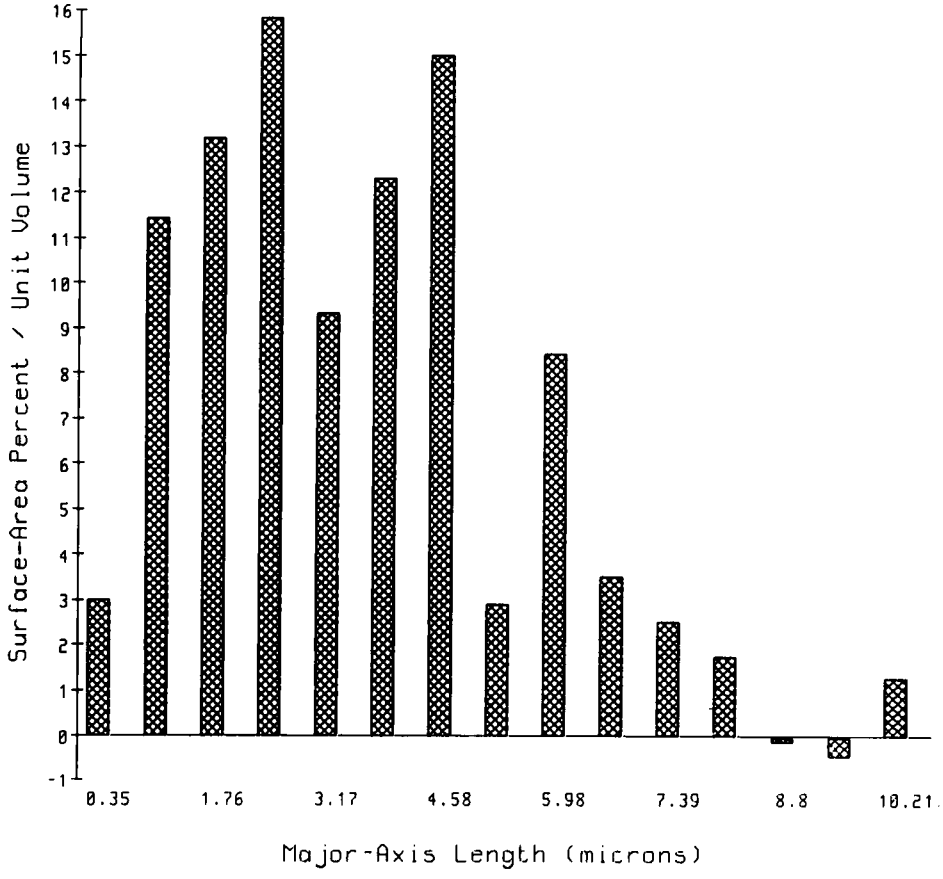

FIGURE 4: Histogram showing the surface area per unit volume for LC droplets as a function of the major-axis length. The distribution is based on results presented in Figure 3 and assumes that the droplets are oblate ellipsoids with the same ratio of minor- to major-axis lengths. The significance of bins with negative contributions is discussed in the text.

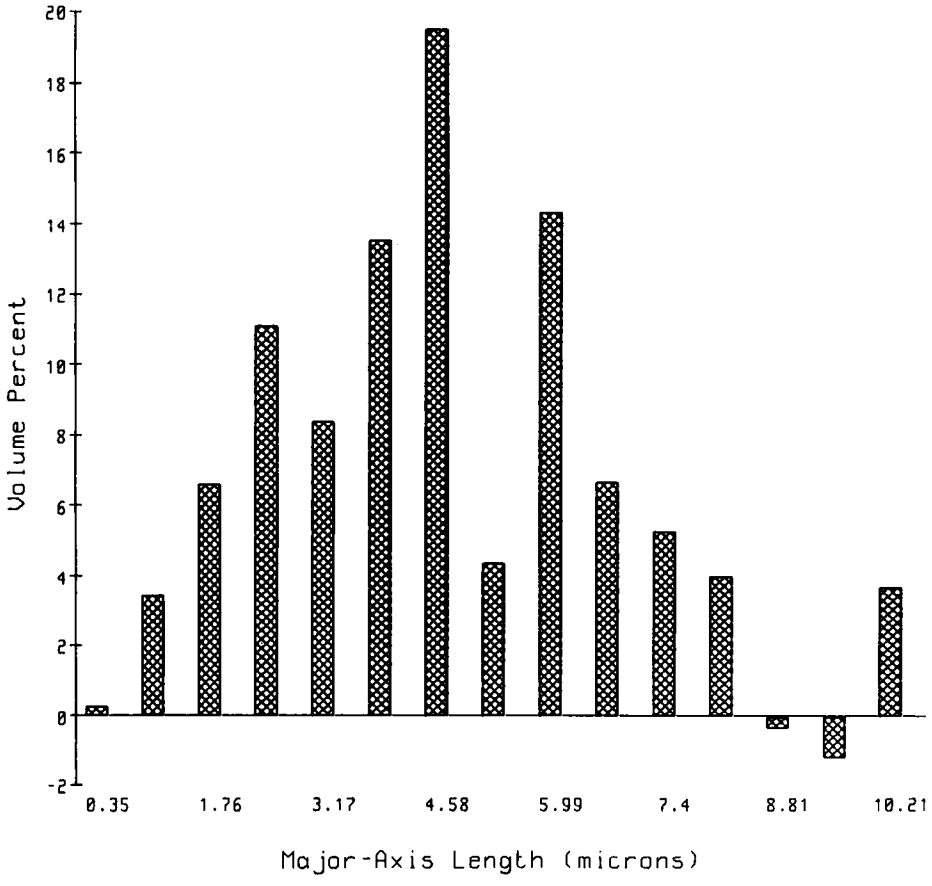

FIGURE 5: Histogram showing the volume distribution for LC droplets, subject to the same assumptions as data in Figure 4.

of the droplets helps to determine the radiation scattering, we anticipate a good correlation between surface area per unit volume and macroscopic scattering efficiency. Of course, with many scattering interfaces separated by variable distances, the scattering model for NCAP films is far from simple.) Standard formulas for the surface area and volume of oblate ellipsoids were used in these calculations[17]; the midpoint of each bin was selected to represent the major-axis length for all particles in that bin. As mentioned earlier, the additional assumption of a uniform q regardless of droplet size was made to facilitate the computation of surface areas and volumes.

Two features of the histograms in Figure 4 and 5 deserve comment: the occasionally large variation in the contributions to adjacent bins and the two bins with negative contributions at major-axis lengths near 9 μm. Both of these are caused by the finite number of droplet sections analyzed. Even though data for a total of 1322 ellipses were tabulated, Figure 3 indicates that in the bins above 5 μm less than 20 droplets contribute to each bin. Because the surface-area and volume distributions involve higher moments of the major-axis length, they are more sen-

sitive to variation in contributions to adjacent bins. This is particularly true for the bins with high major-axis length. (The problem is exacerbated by using a larger number of bins for the same number of droplets.) In the largest bin (centered at 10.21 μm) there is only one droplet, and there are none counted in the two bins just smaller than the largest. Analysis of the summations presented earlier reveals that a large droplet in three dimensions is expected to contribute to all bins in the cross section with major-axis lengths less than or equal to that of the large droplet. However, if there is only one large droplet in the sampling volume, it will yield only one ellipse in the sectioning plane, and this will distort the statistics, leading to phenomena such as negative contributions to particular bins. Therefore, a large sampling area is desirable for this type of quantitative SEM, but must be weighed against the time required to generate representative binary images.

Figure 6 presents the number distribution of droplet sizes per unit volume, as determined by SEM in the NCAP film and by a Coulter Multisizer in the LC

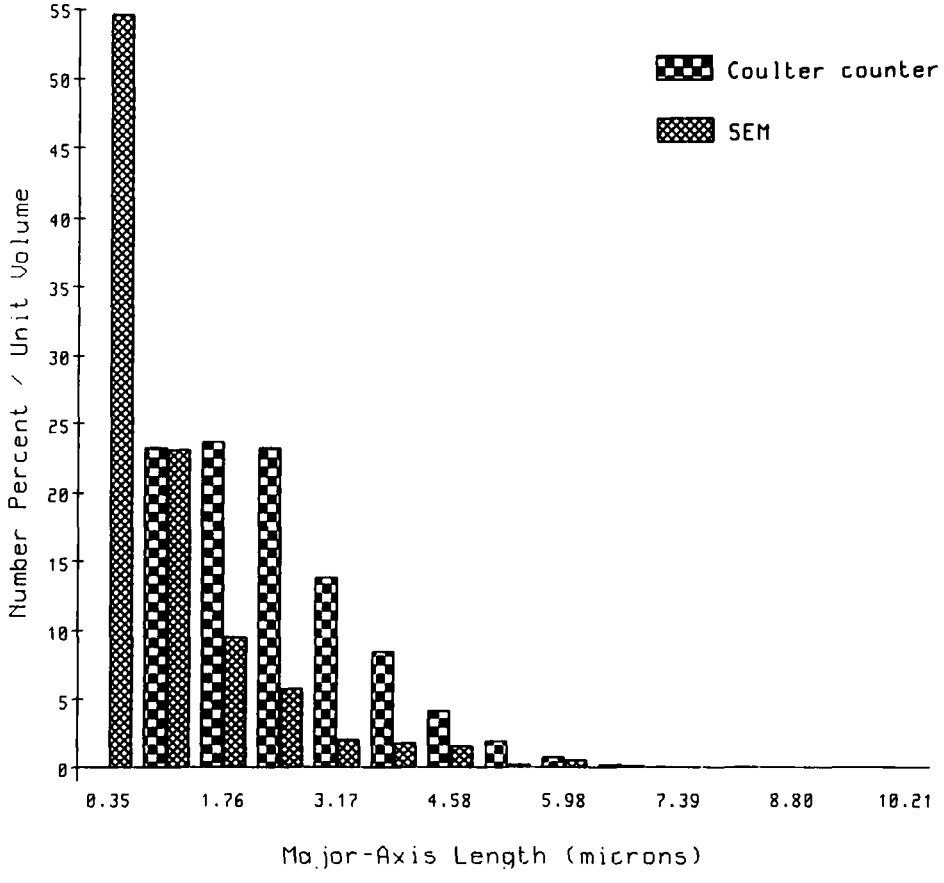

FIGURE 6: A comparison of droplet-size distributions per unit volume from both SEM and Coulter-counter measurements. The latter determines size from impedance measurements on LC emulsions before the films are coated and dried. The SEM results show a much higher fraction of droplets below one micron in size.

emulsion prior to coating. The Coulter Multisizer is a well-known means of particle sizing based on measuring the impedance change as a droplet in the emulsion passes through a small aperture. Its advantages lie in its speed and ease of measurement, as well as in the fact that a few hundred thousand droplets typically contribute to the sample size. Its disadvantages are that droplets in the NCAP film itself are not being analyzed and that its sensitivity to droplet sizes less than one micron is limited for the apertures used in these emulsions. This last point is clear from the data in Figure 6. While the SEM results indicate that the majority of droplets in the film have a major-axis length of less than one micron, the Coulter-counter data tail off in the small-size regime. The volume distributions, as determined by both techniques, are shown in Figure 7. The mean droplet volume is shifted to slightly higher values of the major-axis length for the NCAP film, as expected, since the droplets are oblate ellipsoids in the film and are spheres in the LC emulsion. (For droplets of the same volume, oblate ellipsoids have larger major-axis lengths than do spheres.)

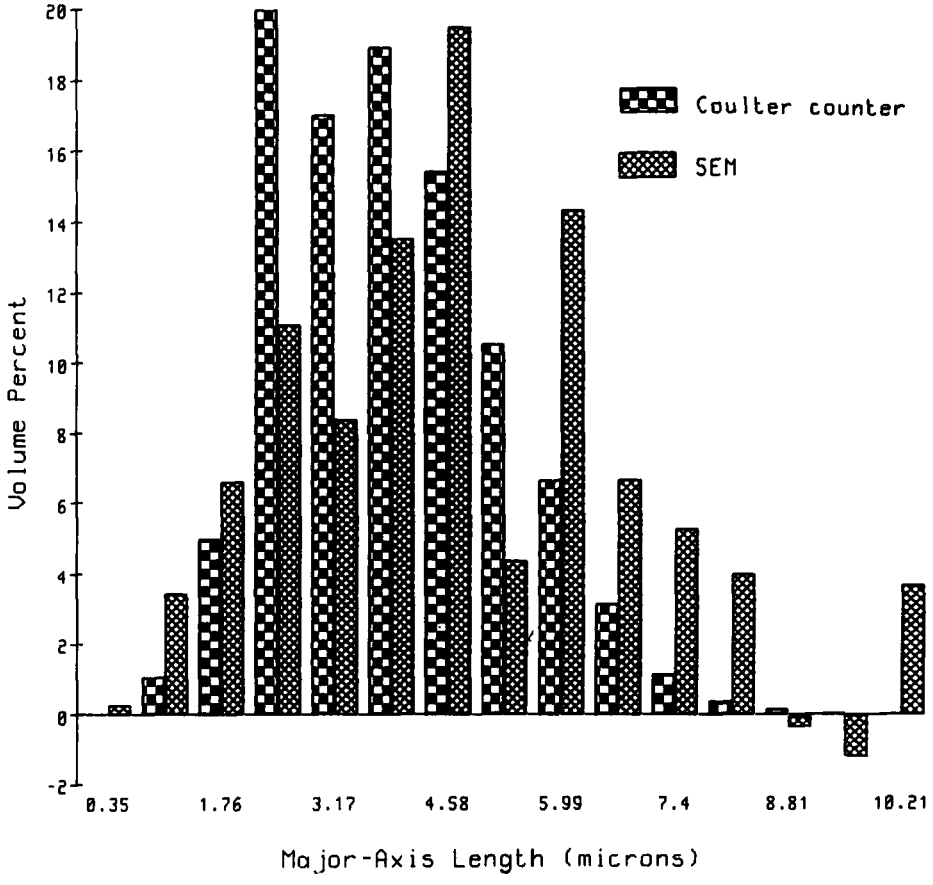

FIGURE 7: A comparison of volume distributions of LC droplets from SEM and Coulter-counter measurements. The increased number of large droplets in the SEM results suggests some droplet coalescence during the coating and drying of the NCAP film.

However, the increased contributions to bins greater than six microns in the NCAP films cannot be accounted for solely by the effect of flattening of the droplets. Here the SEM data suggest that there is some coalescence of the LC droplets as the emulsion is coated onto the electrode. Such changes in size distribution are likely to be sensitive to emulsion-processing procedures and provide a real incentive for quantitative SEM analysis of the NCAP films.

Acknowledgments

The authors gratefully acknowledge the contributions to this work from Chris Coffin, Mark Wartenberg, and Gil Garza of Raychem Corporation.

References

1. J. L. Fergason, *Soc. for Inform. Displays Int. Symp. Dig. Tech. Papers* **16**, 68 (1985).
2. P. S. Drzaic, *J. Appl. Phys.* **60**, 2142 (1986).
3. P. M. Kelly, *Met. Forum* **5**, 13 (1982).
4. M. Blank-Bewersdorff and U. Koester, *Mater. Sci. Eng.* **97**, 313 (1988).
5. U. Koester and P. S. Ho, *Mater. Res. Soc. Symp. Proc.* **77**, 521 (1987).
6. K. C. Dao, *Polymer* **25**, 1527 (1984).
7. R. T. DeHoff, "Quantitative Microstructural Analysis," *Fifty Years of Progress in Metallographic Techniques*, ASTM STP 430, Am. Soc. Testing Mats., 1968, pp. 63–95.
8. R. T. DeHoff, "Quantitative Metallography," *Techniques of Metals Research*, Volume II, Part 1, Interscience, 1968, pp. 221–253.
9. R. T. DeHoff, *Trans. Met. Soc. AIME* **230**, 764 (1964).
10. N. Haroun, *J. Mat. Sci.* **16**, 2257 (1981).
11. R. G. Cortes, A. O. Sepulveda and W. O. Busch, *J. Mat. Sci.* **20**, 2997 (1985).
12. S. Pignolet-Brandom and K. J. Reid, *Proc. 46th Ann. Meeting EMSA*, San Francisco Press, 1988, pp. 674–5.
13. R. T. DeHoff, *Trans. Met. Soc. AIME* **224**, 474 (1962).
14. R. T. DeHoff and F. N. Rhines, *Trans. Met. Soc. AIME* **221**, 975 (1961).
15. E. Scheil, *Z. Metallk.* **27**, 199 (1935).
16. S. A. Saltykov, *Stereometric Metallography*, Second Edition, Metallurgizdat, Moscow, 1958.
17. G. A. Korn and T. M. Korn, *Mathematical Handbook for Scientists and Engineers*, McGraw-Hill Book Company, New York, 1968, p. 883.
18. N. A. Vaz, G. W. Smith and G. P. Montgomery, Jr., *Mol. Cryst. Liq. Cryst.* **146**, 17 (1987).
19. N. A. Vaz, G. W. Smith and G. P. Montgomery, Jr., *Mol. Cryst. Liq. Cryst.* **146**, 1 (1987).
20. J. L. West, *Mol. Cryst. Liq. Cryst.* **157**, 427 (1988).